Polymer Journal (2013) 45, 665–670

www.nature.com/pj

ORIGINAL ARTICLE

# Dynamic holographic images using poly(*N*-vinylcarbazole)-based photorefractive composites

Kenji Kinashi, Yu Wang, Asato Nonomura, Sho Tsujimura, Wataru Sakai and Naoto Tsutsumi

**We present the optimization of poly(*N*-vinylcarbazole) (PVCz)-based photorefractive composite films for use in a dynamic holographic imaging system. The compositions of the composite films used in this study included PVCz/4-azacycloheptylbenzylidenemalononitrile (7-DCST)/carbazoylethylpropionate (CzEPA), *N*-ethylcarbazole, benzyl *n*-butyl phthalate/[6,6]-phenyl-C61-butyric acid methyl ester or 2,4,7-trinitro-9-fluorenone (TNF) (44/35/20/1 wt%). PVCz with molecular weights of 23 000, 100 000, 290 000, 370 000 and 810 000 g mol$^{-1}$ were used. The photorefractive polymeric composite (PPC) film (PVCz with $M_w$: 370 000/7-DCST/CzEPA/TNF, 44/35/20/1 wt%) was observed to be the most well-balanced for photorefractive performance. To demonstrate the practical application of these films, dynamic holographic images were reflected from a spatial light modulator. The optimized PPC film was used in the dynamic holographic imaging system, and well-balanced dynamic holographic images were obtained. The results from this study will contribute to the development of four-dimensional (4D − 3D plus time) holographic displays.**
*Polymer Journal* (2013) **45,** 665–670; doi:10.1038/pj.2012.176; published online 24 October 2012

**Keywords:** dynamic holographic images; photorefractive composites; photorefractive polymers; poly(N-vinylcarbazole)

## INTRODUCTION

The photorefractive effect in polymeric composites includes the formation of a space-charge field through the generation, transport, and trapping of photo-carriers and is followed by a change in the refractive index due to the electro-optic effect and dye reorientation in the space-charge field.[1,2] To better understand the photorefractive effect, both physical and chemical aspects need to be considered. From a physical perspective, the photorefractive effect in organic materials in the dc-field involves the photogeneration of charge carriers in the bright regions of an interference pattern and the subsequent displacement of the mobile charges (typically holes) due to field-induced drift. This charge separation leads to the formation of a periodic internal space-charge field, which is phase-shifted relative to the interference pattern. In materials with low glass-transition temperatures ($T_g$), nonlinear optical dyes are reoriented along the total electric field, which is the vectorial sum of the space-charge field and the applied field. Then, refractive index change results from the linear electro-optic (Pockels) effect and modulated birefringence.[3] The phase shift between the recorded refractive index modulation and the interference pattern gives rise to an asymmetric energy transfer from one writing beam to the other. From a chemical perspective, charge carriers are generated in the bright regions of the interference pattern through the photoexcitation of sensitizers; the given example shows a charge-transfer complex between a photoconductive polymer (that is, poly(*N*-vinylcarbazole) (PVCz)) and a sensitizer (that is, 2,4,7-trinitro-9-fluorenone (TNF)). Subsequently, the mobile holes are transported by the charge-transfer agent from the bright to the dark regions by the applied field, whereas the opposing negative charges remain localized in the bright regions on the electron acceptor sensitizer. Eventually, the holes become trapped in the dark regions and the periodic internal space-charge field accumulates between the bright and dark regions. Finally, the nonlinear optical dye reorients in the total electric field and produces a refractive index grating.

One of the most well-known techniques for producing three-dimensional (3D) displays is holography. Traditional holographic materials, such as dichromated gelatin, silver halides and photopolymers, can be used to create a static (non-updatable) hologram with full-color and full-parallax images. Inorganic crystals ($LiNbO_3$ or $LiTaO_3$),[4] organic glasses,[5,6] liquid crystal systems[7,8] and polymeric composite systems can also be used as materials for dynamic (updatable) holograms. Specifically, photorefractive polymeric composites (PPCs) are the most promising candidates for these various holographic applications. Recent studies have investigated updatable holographic displays[9,10] and all-optical logic gates produced through photorefractive two-wave mixing.[11] The updatable holographic displays developed using photorefractive polymers produced realistic 3D images without requiring special eyeglasses; therefore, the specific characteristics of PPC have recently received considerable attention. The updatable holograph can be recorded in a PPC using two coherent laser beams—the object beam and the reference beam—and then read out by a probe beam to reconstruct the holographic image. Therefore, the simultaneous recording and

Department of Macromolecular Science and Engineering, Kyoto Institute of Technology, Matsugasaki, Sakyo, Kyoto, Japan
Correspondence: Professor N Tsutsumi, Department of Macromolecular Science and Engineering, Kyoto Institute of Technology, Matsugasaki, Sakyo, Kyoto 606-8585, Japan.
E-mail: tsutsumi@kit.ac.jp
Received 14 June 2012; accepted 19 August 2012; published online 24 October 2012

displaying of holograms are rapidly and continuously performed with PPC, which is a potential material for next-generation holographic 3D displays. Currently, commercially available holographic 3D displays that use traditional holographic materials, such as photopolymers lack the image-updating capability, which results in limited used of these displays. To be practically suitable for holographic 3D displays, PPCs require a high diffraction efficiency, fast writing time, rapid erasure, non-aggregation capability and long-term stability.

Here, we study the photorefractive performances of PVCz-based PPC films and develop an optimized PPC film based on the results. Furthermore, we demonstrate that dynamic holographic images can be constructed from a spatial light modulator through the well-balanced PPC film.

## EXPERIMENTAL PROCEDURE

All reagents are commercially available and were used without any further purification. Five types of PVCz with different molecular weights ($M_w$: 23 000, 100 000, 290 000, 370 000 and 810 000 g mol$^{-1}$) were used for the host matrices. 4-Azacycloheptylbenzylidenemalononitrile (7-DCST) was synthesized using procedures described in the literature.[12,13] One of the better known ratios for the the composition of the photorefractive composite was used, which was photoconductive polymer/nonlinear optical dye/plasticizer/sensitizer (44/35/20/1 wt%).[14] PVCz was mixed with 7-DCST, which was used as a nonlinear optical dye; carbazoylethylpropionate (CzEPA), *N*-ethylcarbazole (ECz) and benzyl *n*-butyl phthalate (BBP) as a plasticizer; and [6,6]-phenyl-C61-butyric acid methyl ester (PCBM) and TNF as a sensitizer in a tetrahydrofuran solvent. The mixture was stirred for 24 h and then cast on a hot plate at 70 °C for 24 h. The resulting PPCs were sandwiched between two indium-tin-oxide glass plates at 120 °C, and the PPC films were obtained. The thickness of the PPC films was controlled to be $<100\,\mu m$ using Teflon spacers. The chemical structures of these materials are shown in Figure 1.

The diffraction efficiencies of the PPC films were measured using the degenerate four-wave mixing technique. The holographic gratings were written in the PPC film using two intersected *s*-polarized beams of a He-Ne laser (at 632.8 nm, 10 mW, 1.5 W cm$^{-2}$, LASOS Lasertechnik GmbH, Jena, Germany) at incidence angles of 40.54° and 59.46° in air. A weaker intensity *p*-polarized reading (probe) beam from the same source, which propagated in the direction opposite to the writing beam, was diffracted by the refractive index gratings in the PPC film. Then, the diffracted signal, which was propagated in the direction opposite to another writing beam, was reflected by a beam splitter. The diffracted signal was detected by a photodiode detector. The probe beam that was transmitted through the PPC film was also detected by another photodiode detector. Based on the intensity of the transmitting beam ($I_t$) and the diffracted beam ($I_d$), the diffraction efficiency ($\eta$) was calculated with the following equation:

$$\eta\ \% = \frac{I_d}{I_t + I_d} \times 100$$

A schematic representation of the dynamic holographic imaging process is shown in Figure 2. The dynamic images that were produced by a personal computer were displayed on an spatial light modulator system (1920 × 1200 Holoeye LCR-1080, Berlin-Adlershof, Germany). A semiconductor laser (at 532 nm, 300 mW, 10 mW cm$^{-2}$, Spectra-Physics, Santa Clara, CA, USA) was used for the writing beams (object and reference), which were adjusted to *s*-polarization. In this study, binarized moving images of a running cat were used as a nearly video-rate movie. The dynamic images were reflected by a coherent laser beam, and the reflected laser beam contained the information for the dynamic images that were subsequently illuminated to the PPC film as an object beam. The other branched coherent beam simultaneously lit up toward the illuminated area of the object beam on the PPC film as a reference beam. The recorded dynamic images were simultaneously diffracted by another *p*-polarized semiconductor laser (at 642 nm, 140 mW, 10 mW on the PPC film, Omicron-Laserage, Rodgau-Dudenhofen, Germany) close to the same angle as the reference beam. Finally, the diffracted dynamic images were reconstructed and projected through a color filter onto a screen. At that time, the sample film was maintained under an applied electric field of 40 V μm$^{-1}$.

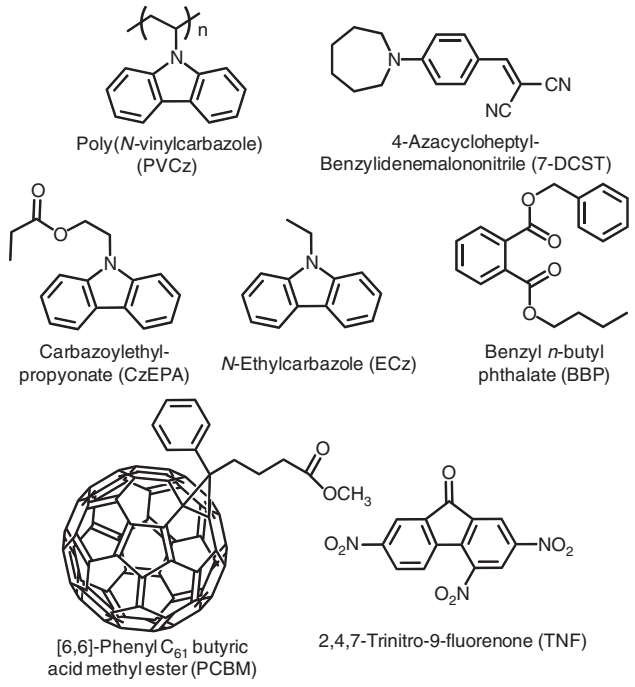


**Figure 1** Chemical structures of the components in the PPCs.

## RESULTS AND DISCUSSION

All of the photorefractive composites with different components, which were at a unified ratio (44/35/20/1 wt%), were investigated using the degenerate four-wave mixing technique. The obtained photorefractive quantities and their glass-transition temperatures ($T_g$) are summarized in Table 1. The diffraction efficiencies ($\eta$) as a function of the applied electric field for all of the PPC films are shown in Figure 3a. The diffraction efficiencies for all of the PPC films increased when the applied electric field was increased. Note that the diffraction efficiencies also tend to increase when the $M_w$ of PVCz increased up to 500 000 g mol$^{-1}$.

The maximum obtained diffraction efficiency was greater than approximately 40% at 45 V μm$^{-1}$ for the PPC films with $M_w$: 370 000. In addition, in the case of $M_w > 1\,000\,000$, the PPC film was difficult to prepare owing to its inflexibility and rigidity. These results imply a strong relationship between the diffraction efficiency and the $M_w$; therefore, a higher diffraction efficiency requires an appropriate $M_w$, $\sim 300\,000 - 600\,000$ g mol$^{-1}$, as shown in Figure 3b. Considerations regarding the increasing tendencies have already been proposed in a previous study.[15] Herein, we provide a brief explanation for why the PVCz with the higher $M_w$'s provides more dominating electro-optic active sites, which is directly related to the higher number density of carrier traps. In a general polymer system, the active end groups in the polymer chain would function as effective carrier traps. In the case of the PVCz system, the dimer cation sites are known to function as active carrier traps. Consequently, the dimer cation sites that predominantly formed along the longer polymer chain in the higher molecular weight PVCz functioned as effective carrier traps.

The effects of using TNF rather than PCBM as a sensitizer on the diffraction efficiency were examined. Consequently, the diffraction efficiency of PVCz with $M_w$: 370 000/7-DCST/CzEPA/TNF was

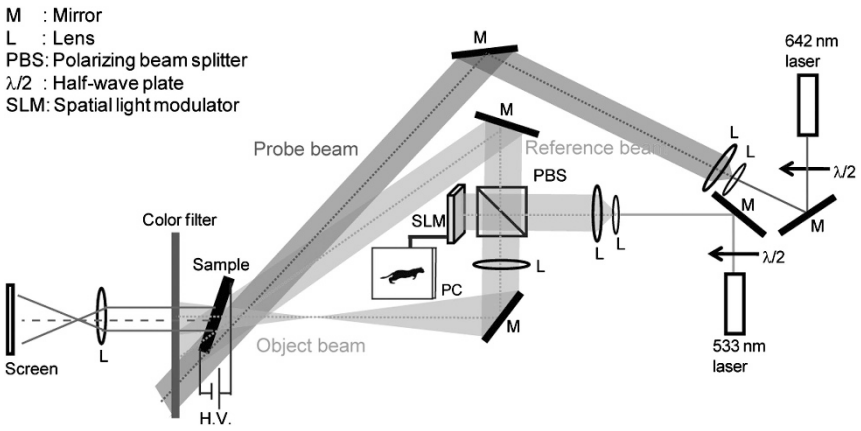


**Figure 2** Experimental setup for the dynamic holographic imaging system. In transmission, two beams (object and reference beams) are used as a writing beam. To observe the images, a probe beam is made to forward-propagate with a reference beam. A diffracted image (red line) passes through a color filter and is projected onto a screen. A full color version of this figure is available at *Polymer Journal* online.

**Table 1 Photorefractive quantities and glass-transition temperatures of the PPC films**

| *PPC, 44/35/20/1* | *PVCz,* $M_w$ | $\eta$ *(%)*[a] | $\tau_{st}$*(ms)*[a] | $T_g$ *(°C)* |
|---|---|---|---|---|
| PVCz/7-DCST/CzEPA/PCBM | 23 000 | 17.4 ± 2.4 | 279 | −28 |
| PVCz/7-DCST/CzEPA/PCBM | 100 000 | 26.2 ± 7.5 | 215 | −26 |
| PVCz/7-DCST/CzEPA/PCBM | 290 000 | 40.0 ± 2.7 | 157 | −15 |
| PVCz/7-DCST/CzEPA/PCBM | 370 000 | 40.2 ± 2.5 | 141 | −10 |
| PVCz/7-DCST/CzEPA/PCBM | 810 000 | 28.4 ± 1.6 | 364 | 2 |
| PVCz/7-DCST/CzEPA/TNF | 370 000 | 63.8 ± 3.6 | 55 | −17 |
| PVCz/7-DCST/ECz/TNF | 370 000 | 34.0 ± 5.1 | 140 | −9 |
| PVCz/7-DCST/BBP/TNF | 370 000 | 17.2 ± 2.2 | 218 | −22 |

Abbreviations: BBP, benzyl *n*-butyl phthalate; CzEPA, carbazoylethylpropionate; 7-DCST, 4-azacycloheptylbenzylidenemalononitrile; ECz, *N*-ethylcarbazole; PCBM, [6,6]-phenyl-C61-butyric acid methyl ester; PVCz, poly(*N*-vinylcarbazole); TNF, 2,4,7-trinitro-9-fluorenone.
[a]Applied electric field at 45 V μm$^{-1}$.

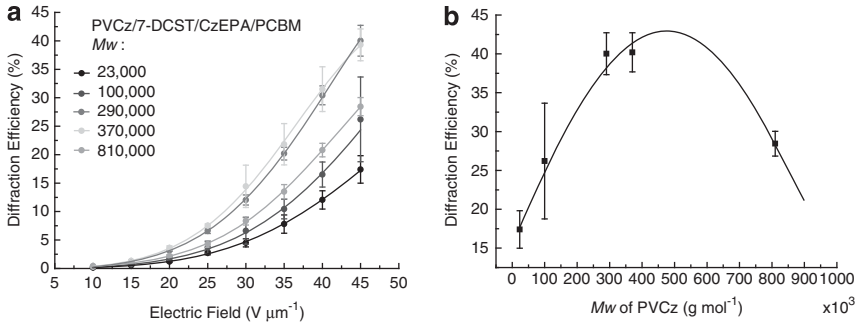


**Figure 3** (**a**) Field dependence of the diffraction efficiency measured in the PPC films. (**b**) Dependence of the diffraction efficiency on the molecular weight. A full color version of this figure is available at *Polymer Journal* online.

~65% at 45 V μm$^{-1}$. The reason for this increased diffraction efficiency can be based on the following report. Wang *et al.*[16] reported that the field-dependent hole mobility of PVCz with a low concentration of fullerene as a dopant had only a small effect on the hole mobility of PVCz. In addition, they mentioned that the introduction of fullerene slightly increased the positional disorder of PVCz, and that the distribution width of the distances between the carbazole groups becomes wider. However, a detailed study on the photogeneration in charge-transfer complexes in PPC films sensitized with fullerene was reported by Hendrickx *et al.*[17] In this work, the authors reported that the use of fullerene as a sensitizer was sufficient for arylamine-based PPC films to yield high hole transport properties.[18] However, PVCz/TNF-based composites show a good hole mobility as a result of the formation of a charge-transfer complex between the TNF and the carbazole units.[19] Accordingly, the use of TNF leads to the high diffraction efficiency for the PVCz-based PPC film.

Next, we examined the effects of three types of plasticizers on the diffraction efficiency, as shown in Figure 4. By changing the plasticizer from CzEPA to ECz (or BBP), the diffraction efficiency decreased

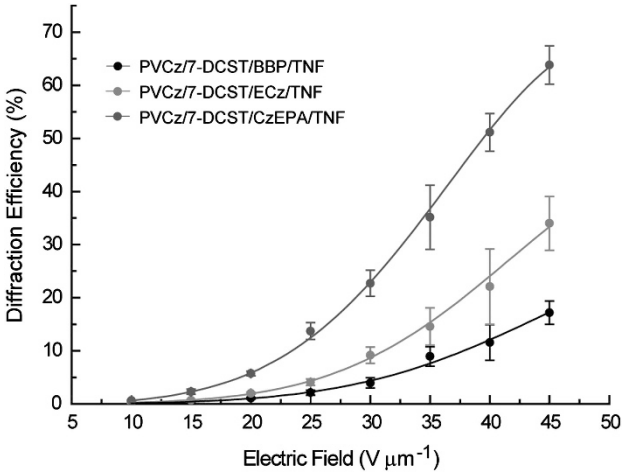


**Figure 4** Dependence of the diffraction efficiency on the plasticizer as a function of the applied field. A full color version of this figure is available at *Polymer Journal* online.

from 65 to 39% (for ECz) and 19% (for BBP). This decreasing tendency was mentioned in our previous report.[20] CzEPA is a carbazole plasticizer and has been confirmed to function as a good photoconductive plasticizer in PVCz-based PPC films because CzEPA functions as an appropriate hole hopping site. In addition, the use of CzEPA significantly decreased the $T_g$ compared with the use of ECz, which increased the orientational enhancement. The improved of diffraction efficiency can also be explained from the results of the photocurrent measurements. Photocurrents of $0.41\,\mu A\,W^{-1}\,cm^{-2}$ (for the use of CzEPA), $0.38\,\mu A\,W^{-1}\,cm^{-2}$ (for the use of ECz), and $0.19\,\mu A\,W^{-1}\,cm^{-2}$ (for the use of BBP) were measured at 632.8 nm ($0.99\,mW\,cm^{-2}$) under an applied electric field of $4\,\mu V\,cm^{-1}$. Therefore, the higher diffraction efficiency of the PPC film plasticized with CzEPA is attributed to the higher photocurrent, which makes it possible to maintain a large density of trapped charges in the matrix. Accordingly, the use of the CzEPA plasticizer led to a higher diffraction efficiency than the other plasticizers.

We discuss the photorefractive response time of these PPC films. The response time of the photorefractive grating recording is an important parameter for practical applications. To determine the time-resolved characteristics of the PPC films, transient degenerate four-wave mixing experiments were performed using a high-speed data acquisition system (count per 0.001 s). The diffraction efficiency as a function of time for the PPC films was measured using the experimental setup described above. At $t=0$, one of the writing beams is unblocked, and the photorefractive response time (grating build-up) is observed at an applied electric field of $45\,V\,\mu m^{-1}$. As an example of the response time, the time profile of the PCBM-sensitized PPC film with $M_w$: 23 000 levels out to ~16% at 600 ms. The analogous PPC films with the other $M_w$'s also exhibit the same response tendency. There have been many suggestions regarding the characterization of the photorefractive dynamics. Among the functions used to fit the refractive response time or two-beam coupling gain measured in the photorefractive experiments are single exponentials,[21,22] bi-exponentials,[23,24] stretched exponentials[25,26] and others. In this study, to understand the details of the response times, the data were fitted to the stretched exponential function of a Kohlrausch–Williams–Watts (KWW) equation as follows:

$$\eta\ \% = \eta_0(1 - \exp(-(t/\tau)^{\beta}))$$

where $\tau$ is the response time, $\beta$ $(0<\beta\leqslant 1)$ is the fitting parameter related to a dispersion that was attributed to the distribution of the release times from the traps, and the electric field dependence of the time constant was explained by the electric-field-assisted release of charges from the trapping sites with a broad energy distribution. The stretched exponential behavior is known to occur when a physical process involves a distribution of time constants with β decreasing as the time constant distribution increases. Figure 5a shows that the best-fit response times of the diffraction efficiencies using the stretched exponential function in the PCBM-sensitized PPC films. The resulting response times are 279 ms (for $M_w$: 23 000), 215 ms (for $M_w$: 100 000), 157 ms (for $M_w$: 290 000), 141 ms (for $M_w$: 370 000) and 364 ms (for $M_w$: 810 000). Consequently, one important characteristic of the time profile is that the overall photorefractive response times in the PCBM-sensitized PPC films increase with an increase in $M_w$; therefore, the response time of the PCBM-sensitized PPC films also requires an appropriate $M_w$ of ~300 000–400 000 g mol$^{-1}$. The dependency of the response times on the plasticizer in the TNF-sensitized PPC films is shown in Figure 5b.

The best-fit response time of the diffraction efficiency using the stretched exponential function in the PPC film plasticized with CzEPA exhibits the fastest response time, 55 ms. When ECz and BBP were used as plasticizers, the best-fit response times were 140 ms and 218 ms, respectively. These results indicate that the PPC films plasticized with ECz and CzEPA formed the charge-transfer complex, which has a good hole mobility; consequently, those response times were relatively faster compared with the others. Therefore, for the PPC film plasticized BBP, the reason for the slow response time is because BBP is a good plasticizer at reducing the $T_g$; however, it cannot form an effective charge-transfer complex as well as the carbazole plasticizers can.

A more noteworthy characteristic is the initial process within 200 ms for the TNF-sensitized PPC films. The bi-exponential function was also used to understand the photorefractive dynamics in more detail. It is well known that a faster component is attributed to the photoconductivity and a slower component to the orientational enhancement.[23]

$$\eta\ \% = \eta_0((1-a)\exp(-(t/\tau_1)) - (1-a)\exp(-(t/\tau_2)))^2$$

where a $(0\leqslant a\leqslant 1)$ is the amplitude of the two exponentials, $\tau_1$ is the faster response time, and $\tau_2$ is the slower response time. The best-fit time constants of the bi-exponential function and their contributions to the profiles of the TNF-sensitized PPC films are as follows: $\tau_1$: 24 ms (88%), $\tau_2$: 319 ms (12%) for PPC6; $\tau_1$: 62 ms (85%), $\tau_2$: 630 ms (15%) for PPC7 and $\tau_1$: 79 ms (72%), $\tau_2$: 651 ms (28%) for PPC8. The average response times were calculated to be 59 ms for PPC6, 147 ms for PPC7 and 239 ms for PPC8. Unfortunately, for the PCBM-sensitized PPC films, the bi-exponential fitted response times were not in agreement with the stretched exponential response times. Note that the faster response times ($\tau_1$) in the PPCs were relatively fast in the range of 24–79 ms, and that contributions are ~80%. Accordingly, all of the TNF-sensitized PPCs exhibited a remarkable improvement for the contribution of faster response times ($\tau_1$). It is thus suggested that the faster component is attributed to the photoconductivity of the charge-transfer complex. Therefore, the use of CzEPA and TNF can provide completely well-balanced photorefractive performances for the PVCz-based PPC film.

Practical applications of dynamic holographic imaging are presented in the following. Several snap-shots of dynamic holographic images at an interval of 1 s were projected onto a screen that was reconstructed by the optimized PPC film (PPC6), as shown in

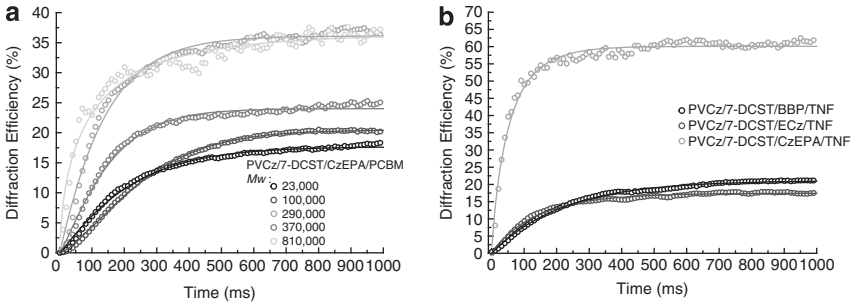


**Figure 5** Diffraction efficiency as a function of time for the PPC films at various molecular weights (**a**) and plasticizers (**b**) showing photorefractive response time. At time zero, the writing beams were turned on. The data were fitted to the stretched exponential function. A full color version of this figure is available at *Polymer Journal* online.

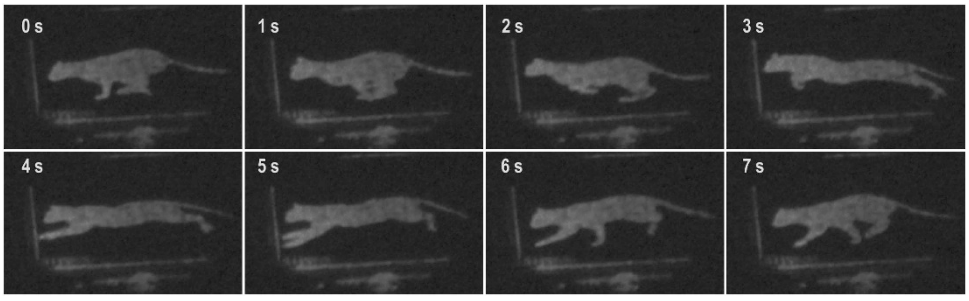


**Figure 6** Photographs showing dynamic holographic images via the PPC film ($M_w$: 370 000 of PVCz, 7-DCST, CzEPA and TNF, 44/35/20/1 wt%) at 1 s intervals (Media 1; Supplementary information). A full color version of this figure is available at *Polymer Journal* online.

Figure 6. At that time, the optimized PPC film was maintained under an applied electric field at 40 V μm$^{-1}$. The updated dynamic image on the spatial light modulator was clearly projected onto the screen as a dynamic hologram using the optimized PPC film. The holographic images clearly reconstructed the original motion of the front paws of a cat with a quick response. In the case of stop motion, the bright holographic images were precisely reconstructed: the image could be immediately stopped without blurring. From these results and observations, high diffraction efficiency, fast response time and fast rising at an initial time within 100 ms are required for updatable 3D imaging.

## CONCLUSIONS

In this study, we have investigated the effects of the PVCz molecular weight and the use of different plasticizers and sensitizers on the photorefractive parameters of PPC films. Consequently, the PPC film with appropriate additives ($M_w$: 370 000 of PVCz, 7-DCST, CzEPA and TNF, 44/35/20/1 wt%) has a well-balanced photorefractive performance. Dynamic images were projected onto a screen at an interval of 1 s and were clearly reconstructed by the best PPC film. Note that the best PPC film can clearly follow the original motion of a movie produced on a computer with a quick response quality. Consequently, the well-balanced PPC is a suitable option for a dynamic holographic imaging system.

In the future, we will undertake a study to demonstrate updatable holographic imaging using PVCz-based PPC film with well-balanced performance. The use of computer generated holograms is required to achieve holographic displays because computer-generated holograms can create holograms not only of single objects but also of full scenes with multiple dynamic objects.[27,28] However, this task is extremely difficult due to the considerable computational programming and time requirements, and the results are often of poor quality in terms of image resolution. Regardless, we believe that full-color, full-parallax, real-time holographic displays will benefit from the use of computer generated holograms.

## ACKNOWLEDGEMENTS

We thank Mr Iwai and Mr Urata, Nippon Shokubai, for preparing $M_w$: 23 000 of PVCz and CzEPA. This work is supported in part by the program for Strategic Promotion of Innovative Research and Development (SPIRE), Japan Science and Technology Agency (JST).

1 Zilker, S. J. Materials design and physics of organic photorefractive systems. *Chem. Phys. Chem.* **1,** 72–87 (2000).
2 Moerner, W. E. & Silence, S. M. Polymeric photorefractive materials. *Chem. Rev.* **94,** 127–155 (1994).
3 Bittner, R. & Meerholz, K. in *Photorefractive Materials and their Applications II: Materials,* Springer Series in Optical Science (eds Günter, P. & Huignard, J. -P.) (Springer, Berlin, 2006).
4 Petrov, M. P., Stepanov, S. I. & Khomenko, A. V. in *Photorefractive Crystals in Coherent Optical Systems*, Springer Series in Optical Sciences (Springer-Verlag, Berlin, 1991).
5 Ducharme, S., Scott, J. C., Twieg, R. J. & Moerner, W. E. Observation of the photorefractive effect in a polymer. *Phys. Rev. Lett.* **66,** 1846–1849 (1991).
6 Würthner, F., Wortmann, R. & Meerholz, K. Chromophore design for photorefractive organic materials. *Chem. Phys. Chem.* **3,** 17–31 (2002).
7 Wiederrecht, G. P., Yoon, B. A. & Wasielewski, M. R. High photorefractive gain in nematic liquid crystals doped with electron donor and acceptor molecules. *Science* **270,** 1794–1797 (1995).
8 Ono, H., Shimokawa, H., Emoto, A. & Kawatsuki, N. Effects of droplet size on photorefractive properties of polymer dispersed liquid crystals. *Polymer (Guildf)* **44,** 7971–7978 (2003).
9 Tay, S., Blanche, P. -A., Voorakaranam, R., Tune, A. V., Lin, W., Rokutanda, S., Gu, T., Flores, D., Wang, P., Hilaire, St. P., Thomas, J., Norwood, R. A., Yamamoto, M. &

Peyghambarian, N. An updatable holographic three-dimensional display. *Nature* **451,** 694–698 (2008).
10 Blanche, P. -A., Bablumian, A., Voorakaranam, R., Christenson, C., Lin, W., Gu, T., Flores, D., Wang, P., Hsieh, W. -Y., Kathaperumal, M., Rachwal, B., Siddiqui, O., Thomas, J., Norwood, R. A., Yamamoto, M. & Peyghambarian, N. Holographic three-dimensional telepresence using large-area photorefractive polymer. *Nature* **468,** 80–83 (2010).
11 Ishikawa, D., Okamoto, A., Honma, S., Ito, T., Shimayabu, K. & Sato, K. All-optical multifunctional logic gates for image information using photorefractive two-wave mixing. *Opt. Rev.* **14,** 246–251 (2007).
12 Díaz-García, M. A., Wright, D., Casperson, J. D., Smith, B., Glazer, E., Moerner, W. E., Sukhomlinova, L. I. & Twieg, R. J. Photorefractive properties of poly(*N*-vinyl carbazole)-based composites for high-speed applications. *Chem. Mater.* **11,** 1784–1891 (1999).
13 Kinashi, K., Lee, K. -P., Matsumoto, S., Ishida, K. & Ueda, Y. Alkyl substituent effects on J- or H-aggregate formation of bisazomethine dyes. *Dyes Pigments* **92,** 783–788 (2012).
14 Tsutsumi, N. & Kasaba, H. Effect of molecular weight of poly(*N*-vinyl carbazole) on photorefractive performances. *J. Appl. Phys.* **104,** 073102 (2008).
15 Tsutsumi, N., Kinashi, K. & Sakai, W. in *Polymer Photonics, and Novel Optical Technologies* (eds Kawabe, Y. & Kawase, M.) (Photonics World Consorsium Publishing, 2011).
16 Wang, Y. & Suna, A. Fullerenes in photoconductive polymers. charge generation and charge transport. *J. Phys. Chem. B* **101,** 5627–5638 (1997).
17 Hendrickx, E., Kippelen, B., Thayumanavan, S., Marder, S. R., Persoons, A. & Peyghambarian, N. High photogeneration efficiency of charge-transfer complexes formed between low ionization potential arylamines and $C_{60}$. *J. Chem. Phys.* **112,** 9557–9561 (2000).
18 Hendrickx, E., Zhang, Y. D., Ferrio, K. B., Herlocker, J. A., Anderson, J., Armstrong, N. R., Mash, E. A., Persoons, A. P., Peyghambarian, N. & Kippelen, B. Photoconductive properties of PVK-based photorefractive polymer composites doped with fluorinated styrene chromophores. *J. Mater. Chem.* **9,** 2251–2258 (1999).
19 Ramos, G., Belenguer, T. & Levy, D. A highly photoconductive poly(vinylcarbazole)/2,4,7-trinitro-9-fluorenone sol –gel material that follows a classical charge-generation model. *J. Phys. Chem. B* **110,** 24780–24785 (2006).
20 Tsutsumi, N. & Miyazaki, W. Photorefractive performance of polycarbazoylethylacrylate composites with photoconductive plasticizer. *J. Appl. Phys.* **106,** 083113 (2009).
21 Ostroverkhova, O., Moerner, W. E., He, M. & Twieg, R. J. Role of temperature in controlling performance of photorefractive organic glasses. *Chem. Phys. Chem.* **4,** 432–744 (2003).
22 Ostroverkhova, O., Moerner, W. E., He, M. & Twieg, R. J. High-performance photorefractive organic glass with near-infrared sensitivity. *Appl. Phys. Lett.* **82,** 3602–3604 (2003).
23 Ostroverkhova, O. & Singer, K. D. Space-charge dynamics in photorefractive polymers. *J. Appl. Phys.* **92,** 1727–1743 (2002).
24 Herlocker, J. A., Ferrio, K. B., Hendrickx, E., Guenther, B. D., Mery, S., Kippelen, B. & Peyghambarian, N. Direct observation of orientation limit in a fast photorefractive polymer composite. *Appl. Phys. Lett.* **74,** 2253–2255 (1999).
25 Ostroverkhova, O., Gubler, U., Wright, D., Moerner, W. E., He, M. & Twieg, R. Recent advances in understanding and development of photorefractive polymers and glasses. *Adv. Funct. Mater.* **12,** 621–629 (2002).
26 Kador, L., Bausinger, R., Leopold, A., Haarer, D. & Kohler, W. Relaxation dynamics of cascaded linear processes. *J. Phys. Chem. A* **108,** 1640–1643 (2004).
27 Huebschman, M. L., Munjuluri, B. & Garner, H. R. Dynamic holographic 3-D image projection. *Opt. Express* **11,** 437–445 (2003).
28 Paturzo, M., Memmolo, P., Finizio, A., Näsänen, R., Naughton, T. J. & Ferraro, P. Synthesis and display of dynamic holographic 3D scenes with real-world objects. *Opt. Express* **18,** 8806–8815 (2010).

Supplementary Information accompanies the paper on Polymer Journal website (http://www.nature.com/pj)